

11-37  
53335  
7-1

NASA Contractor Report 187130

# On Representation of Mechanical Behavior and Stereological Measures of Microstructure

E.T. Onat and S.I. Wright  
*Yale University*  
*New Haven, Connecticut*

June 1991

Prepared for  
Lewis Research Center  
Under Grant NAG3-834



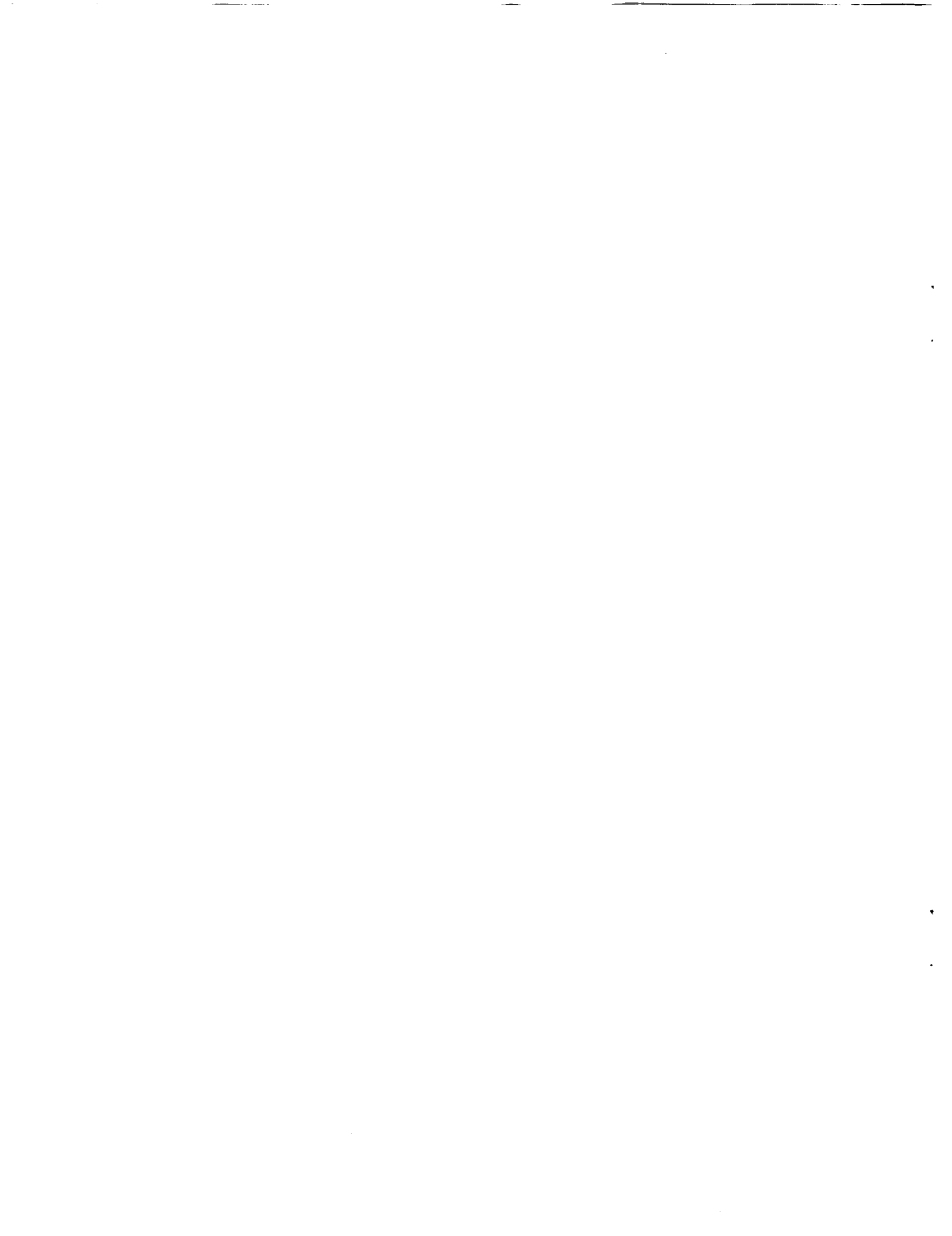
(NASA-CR-187130) ON REPRESENTATION OF  
MECHANICAL BEHAVIOR AND STEREOLOGICAL  
MEASURES OF MICROSTRUCTURE: Final Report  
(Yale Univ.) 21 p

N91-25436

CSCL 20K

Unclass  
C020335

53/59



# ON REPRESENTATION OF MECHANICAL BEHAVIOR AND STEREOLOGICAL MEASURES OF MICROSTRUCTURE

E.T. Onat and S.I. Wright  
Yale University  
Department of Mechanical Engineering  
New Haven, Connecticut 06520

## Summary

Macroscopic homogeneity of a heterogeneous body is defined from various points of view. The applicability of the principle of Delesse to a single macroscopically homogeneous body is discussed. It is then seen that a function derived from a consideration of the area fraction of a phase can serve as a measure of clustering of particles of that phase.

## 1. Introduction

A fundamental task of the engineer is to predict the behavior of a structure composed of a given material under extreme operating conditions. The structure may be a piece of material undergoing a forming operation or a turbine disk or a part of a space vehicle.

With this task in mind, phenomenological and microscopic studies are conducted on the mechanical behavior of the material of interest. The material will, as a rule, exhibit heterogeneities at various scales of magnification. For the sake of simplicity consider here the case where the material can be taken to be a *heterogeneous* continuum. Let this continuum be in a state of equilibrium at temperature  $\theta_0$ .

To conduct an isothermal *phenomenological* (thought) *experiment* we may extract a spherical element of radius  $R$  from the material and apply to its *boundary* a time dependent homogeneous deformation  $F(\tau)$  while keeping the boundary temperature at  $\theta_0$ . Here  $\tau \geq 0$  denotes the time and  $F$  is a linear invertible map on  $\mathbb{R}^3$  with  $F(0) = I$ . The deformation applied to the boundary will cause the development of stresses within the element and these stresses will vary from point to point because of the assumed heterogeneity of the material. Let  $\sigma(\tau)$  denote the *average* of this field over the element at time  $\tau$  (Note that  $\sigma(0) = 0$ ).

The relationship  $\Phi$  that exists, for a given element of the material, between the histories of applied deformation  $F(\tau)$  and the observed average stress  $\sigma(\tau)$  is of great interest to the engineer and material scientist.

The applied deformation will be accompanied by changes that take place in the internal structure of the element. Indeed, it is these changes that impose the relationship  $\Phi$  on the mechanical behavior. Hence, the need for microscopic studies of internal structure at various stages of a phenomenological experiment.

It must be emphasized that the relationship  $\Phi$  will depend, because of the assumed heterogeneity of the material, not only on the constituents and internal structure of the material but also on the radius  $R$  and the location  $\mathbf{x}_C$  of the center of the element that was extracted from the material:

$$\Phi = \Phi(\mathbf{x}_C, R)$$

Suppose that the relationship  $\Phi(\mathbf{x}_C, R)$  ceases to depend on  $\mathbf{x}_C$  as  $R$  increases and tends to the limit  $\Phi_0$ . In other words, if, for every  $\epsilon > 0$ , there exists a minimal radius  $R_\epsilon$  such that

$$R > R_\epsilon \text{ implies } \rho(\Phi(\mathbf{x}_C, R), \Phi_0) < \epsilon$$

where  $\rho$  is a function that measures the “distance” between two constitutive relationships<sup>1</sup>, then we say that the material is *macroscopically homogeneous* from the point of view of mechanical behavior.

If for a desirable  $\epsilon$  the minimal radius  $R_\epsilon$  is much smaller than some of the characteristic lengths associated with the structure, loading, etc., one can, for purposes of structural analysis, replace the actual heterogeneous material with one which is homogeneous and exhibits the constitutive relationship  $\Phi_0$ . On the other hand, in some materials such as manufactured composites the size of the elements of the hard phase is usually much larger than, say, the grain size so that  $R_\epsilon$  may, in some cases, exceed characteristic lengths associated with the structure and loading. In such a case the classical continuum analysis of the structure needs to be supplemented by appropriate modifications.

The next task is to develop constitutive equations that reproduce, *with various levels of accuracy*, the “homogenized” mechanical behavior  $\Phi_0$ . The engineer will then choose from this set constitutive equations that are appropriate to the problem at hand and will use these equations, together with the conservation laws of mechanics and appropriate numerical techniques to obtain the fields of average stress, strain, temperature, etc. over the structure.

---

<sup>1</sup> For a definition of distance between behaviors see Geary and Onat (1974).

Most of the recent work on the (approximate) representation of mechanical behavior  $\Phi_0$  can be put in the following “canonical” form (cf. Geary and Onat (1974)) based on the notion of *state and orientation*:

$$\begin{aligned} \sigma(t) &= f(S(t)) & f: \Sigma \rightarrow T_2^s, \Sigma \subset \mathbb{R}^N \\ \frac{dS(t)}{dt} &= g(S, D) + T_\Omega S(t) & g: \Sigma \times T_2^s \rightarrow \mathbb{R}^N \end{aligned} \quad (1)$$

where suitable initial conditions and invariance requirements imposed on the functions of  $f$  and  $g$  are omitted for simplicity.

It should be pointed out immediately that (1) is appropriate for isothermal deformations of non-aging *solids* and, as noted above, is valid only for material elements that are *sufficiently large*.

In (1),  $\sigma(t)$  denotes the *average* Cauchy stress carried by the material element at time  $t$  and  $T_2^s$  denotes the space of symmetric second rank tensors.  $D$  and  $\Omega$  are, respectively, the tensors of rate of deformation and rotation at that time defined as follows:

$$\dot{F}(t)F^{-1}(t) = D + \Omega \quad (2)$$

where  $F$  is the homogeneous deformation applied to the boundary of the element and the dot denotes derivative with respect to time.

$S(t)$  stands for the  $N$  parameters that measure those aspects of the present microstructure within a sufficiently large material element ( $R \geq R_c$ ) that are relevant to an (approximate) description of the future mechanical behavior of the element. We refer to  $S$  as the *internal state and orientation of the material*; although, we recognize that  $S$  cannot describe all the details of the microstructure if  $N$  is not extremely large.

The first equation above simply states that the current stress follows from the knowledge of the current state and orientation  $S$  of the material. Most materials of interest suffer changes in their internal structure as they deform. The second equation of (1) is a statement as to how these changes take place. Note that  $\dot{S}$ , the rate of change of the state and orientation of the material, depends only on the present  $S$  and on the current values of the rates of deformation and rotation,  $D$  and  $\Omega$ . Moreover, the dependence of  $\dot{S}$  on  $\Omega$ , as is implied by the second equation in (1), is of a very special kind. An important part of the law of evolution for  $S$  comes from a consideration of the role played by superimposed rigid body rotations. It is then seen (Geary and Onat (1974)) that the  $N$  parameters that measure the state and orientation of the material element arrange themselves to form *irreducible* tensors:

$$\mathbf{S} = (q_1, q_2, \dots, q_n).$$

Irreducible tensors serve as measures of symmetry, and tensorial state variables with rank higher than zero make their appearance when the material is anisotropic or when it develops anisotropy during the course of deformation.

Clearly the engineer would like to know the answers to the following questions :

- (i) For a given macroscopically homogeneous material, what is the minimum radius  $R_\epsilon$  which renders the mechanical behavior of a spherical element independent, to within an error  $\epsilon$ , of the location and size of the element ?
- (ii) What aspects of the present microstructure strongly influence the future mechanical behavior and how can these aspects be incorporated into the representation (1)?

In the present paper, we begin a study of these questions for the simple case of a two phase material where each phase is composed of a homogeneous continuum. (It will be appreciated that such a material may be a satisfactory model for certain composites, granular media, and damaged continua).

Clearly, the mechanical behavior of such a material will depend not only on the behavior of its constituents but also on the volume fraction and on the geometrical arrangement of these constituents. For instance, consider the classical case where one of the phases is stiff and the other is ductile. If the microstructure is such that one can find planes that do not intersect the hard phase then the contribution of the hard phase to the stiffness of the composite could be negligibly small. On the other hand, in granular media the elements of the hard phase may align themselves to form *connected substructures* during the course of deformation and this would give rise to a great increase in the stiffness of the material.

A purpose of the paper is to investigate the relevance of stereological measures of microstructure (volume, area and line fractions) to the questions raised above. Another purpose of the paper is to reconsider the celebrated principle of Delesse of the field of Stereology without using the notion of an ensemble and the ergodic hypothesis.

## 2. Stereological Measures of Microstructure

We consider the simple case of a *planar* body that extends to infinity. The body is composed of two homogeneous phases which we shall call black and white. We shall assume that the black

phase occupies an *open* set of  $\mathbb{R}^2$  and the white phase is assigned to the complement of this set. An example of such a body is shown in Fig. 1.

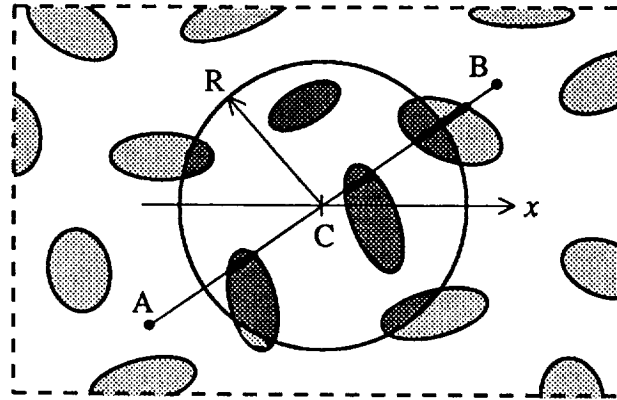


Figure 1. Two phase body sampled by a line segment and a circular area.

Two stereological measures of the microstructure of this planar body are the area and length fractions, say, of the black phase. These are respectively  $A_b/A$  and  $l_b/l$  where  $A_b$  is the total area of the black phase found in a circle of radius  $R$  centered at  $C$ ,  $A = \pi R^2$  and  $l_b$  is the total length of the black segments found on the segment  $AB$  of length  $l$  (cf. Fig. 1).

Let  $C$  be the mid-point of this segment and  $\theta$  the angle the line segment makes with the horizontal axis  $x$ . Clearly, for a given body, the length fraction is a function of the arguments shown below

$$\frac{l_b}{l} = f_1(x_C, \theta; l) \quad (3)$$

where  $x_C$  is the position vector of  $C$ . Similarly,

$$\frac{A_b}{A} = f_2(x_C; R) \quad (4)$$

The functions  $f_1$  and  $f_2$  are easily measurable signatures of the microstructure.

In a *macroscopically homogeneous* body the area fraction  $f_2$  will cease to depend on  $x_C$  and will tend to the constant value  $a_b$  (the area fraction of the black phase) as  $R$  increases. In more formal language, we say that a body composed of two phases is *macroscopically homogeneous* from the point of view of its constituents, if there exists, for any  $x_C$  and  $\epsilon > 0$ , a *minimal*  $R'_\epsilon > 0$  such that

$R > R'_\epsilon$  implies  $|A_b/A - a_b| < \epsilon$  where  $a_b$  is a constant. Thus the area fraction of the black phase within a circular observation window differs from the area fraction  $a_b$  of the material by less than an error of  $\epsilon$ , if the window has a radius  $R'_\epsilon$  or larger.

For a given material,  $R'_\epsilon$  will be a function of  $\epsilon$ :

$$R'_\epsilon = r(\epsilon)$$

We shall see below that two macroscopically homogeneous microstructures that have the same area fraction  $a_b$  may give rise to functions  $r_1(\epsilon)$  and  $r_2(\epsilon)$  that differ from each other by an order of magnitude, for a given  $\epsilon$ .

We point out that the previously introduced  $R_\epsilon$  is different from  $R'_\epsilon$  in that  $R_\epsilon$  renders the mechanical behavior independent of  $x_C$  to within an error of  $\epsilon$ , whereas  $R'_\epsilon$  does the same for the area fraction. However, we expect that  $R_\epsilon$  will be related to  $R'_\epsilon$  in the following sense: consider two materials that have the same area fraction  $a_b$ . If  $r_1(\epsilon) \gg r_2(\epsilon)$  for these two materials, then we will also have  $R_{\epsilon}^{(1)} \gg R_{\epsilon}^{(2)}$ . Hence, our interest in the function  $r(\epsilon)$ . We shall say more about this function in the concluding Section of the paper.

The line fraction function  $f_1$  gives more detailed information on the microstructure of the material. For instance the fact that a given microstructure has preferred directions will be discernable from the  $\theta$  dependence of  $f_1$ .

The question arises: in a macroscopically homogeneous body will  $f_1$  also cease to depend on its arguments  $\theta$  and  $x_C$  as  $l$  increases? A naive interpretation of the principle of Delesse<sup>2</sup> (1847) (which states that in a multi-phase material, the volume(area) fraction of a particular phase is equal to the area (line) fraction of the phase contained in a planar (line) cut through the volume (area)) would suggest that this would be the case and moreover we would have

$$\lim_{l \rightarrow \infty} f_1 = \lim_{R \rightarrow \infty} f_2 \quad (5)$$

It will be remembered, however, that the quantities such as volume fraction that appear in the principle of Delesse refer to the average of measurements made in the neighborhood of a point over an ensemble of samples of the material, whereas in the laboratory and as in the present paper one works with a single body and one makes measurements over subareas and segments of the body.

---

<sup>2</sup> The principle was originally derived for volume and area fractions. Rosiwal (1898), Thomson (1930) and Glagolev (1933) extended it to lower dimensions (cf. Weibel (1980)).

Thus, it is not surprising that, as the example considered below shows, the assertion (3) does not hold for certain microstructures. However a weaker version of (3), (cf. (9)), is valid for all macroscopically homogeneous bodies.

We shall now discuss, in terms of simple examples, the various issues raised above, such as appropriate size of an observation window and the validity and usefulness of the principle of Delesse for measurements performed over a single body.

### 3. Example: Periodic Checkerboard

As the first example we consider a two dimensional body which extends to infinity and has the periodic structure of a regular checkerboard shown in Fig. 2. The body is generated by the repeated application of translations of  $2e_1$  and  $2e_2$  (where  $e_1$  and  $e_2$  are mutually orthogonal unit vectors) to the following cell:

$$\text{cell: } \left\{ \begin{array}{l} \text{Black: when } (x,y) \in B = \left\{ (x,y): \begin{array}{l} 0 < x \text{ and } y < 1, \text{ and} \\ 1 < x \text{ and } y < 2 \end{array} \right\} \\ \text{White: when } (x,y) \in \{(x,y): 0 \leq x \text{ and } y \leq 2\} - B \end{array} \right\} \quad (6)$$

This results in the following checkerboard pattern:

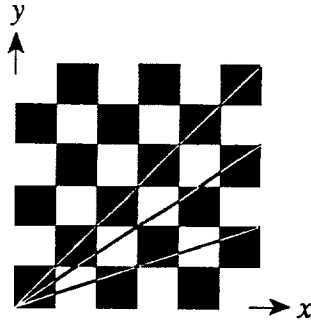


Figure 2. Checkerboard cut with the lines:  
 $y = mx, m = 1, 2/3$  and  $1/3$ .

#### Area Fraction

We now study, in this two phase material, the dependence of the *area fraction*  $A_b/A$  on the center  $x_C$  and the radius  $R$  of the measuring circle.

It is easily seen that as  $A = \pi R^2$  increases,  $A_b/A$  becomes nearly independent of the location and the radius of the circle and approaches  $1/2$ . Thus, in the language introduced before, there exists, for any  $\epsilon > 0$ , a minimal  $R'_\epsilon > 0$  such that  $R > R'_\epsilon$  implies  $|A_b/A - 1/2| < \epsilon$  for any  $x_C$ .

We are interested in the function  $r(\epsilon)$  which depicts the  $\epsilon$  dependence of  $R'_\epsilon$ . Although in the present simple case this dependence can be studied analytically, we prefer here a computational

approach that can be used for more complicated internal structures. Thus, we calculate  $|A_b/A - 1/2|$ , for some  $(x_C, R)$  circle and represent the resulting pair  $(|A_b/A - 1/2|, R)$  by a point in Fig. 3a. The “cloud” of open circles in this figure represents the results of many such calculations. It is then easily seen that the graph of  $r(\varepsilon)$  (with the  $|A_b/A - 1/2|$  axis now serving as the  $\varepsilon$ -axis) will coincide with the “right” boundary of this cloud if the graph of the boundary is a monotonically decreasing function of  $\varepsilon$ . Otherwise  $r(\varepsilon)$  will exhibit discontinuities and its graph will consist of certain monotonically decreasing parts of this boundary.

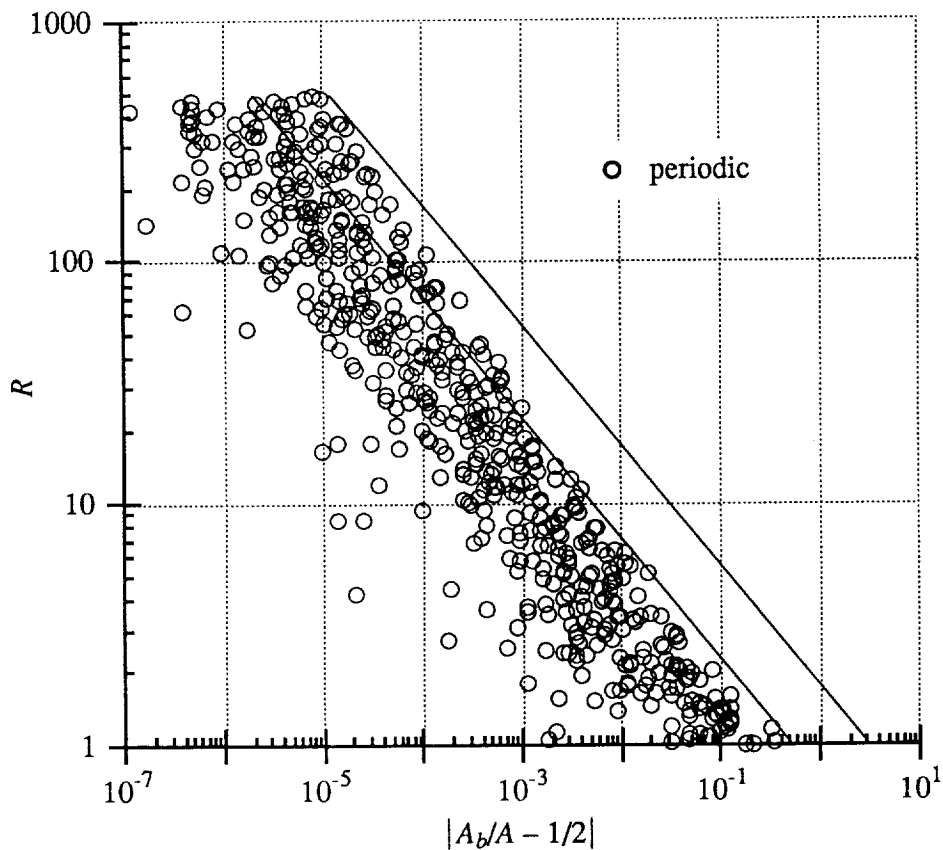


Fig 3.a. Plot of  $(|A_b/A - 1/2|, R)$  pairs for periodic checkerboard.

In this figure the oblique line on the left represents the equation

$$R^2 \varepsilon = 1/2 \tag{7}$$

which, as a simple analysis will show, describes, for *square* domains of observation, the asymptotic behavior of the function  $r(\epsilon)$  as  $\epsilon \rightarrow 0$ . The second line is parallel to the first one and is drawn for comparison of asymptotic behaviors. We see from Fig. 3a that a measurement with radius  $R \geq 5$  is needed to obtain the area fraction of the black phase to within an error of 0.01.

Somewhat similar calculations were performed for the *random* checkerboard considered in Section 4 which also has the area fraction  $1/2$ . Fig. 3b represents the results of these calculations. The two oblique lines of Fig. 3a are added to this figure for purposes of comparison. We see that a much larger radius, namely  $R \geq 50$ , is now needed to estimate the area fraction to within an error of 0.01.

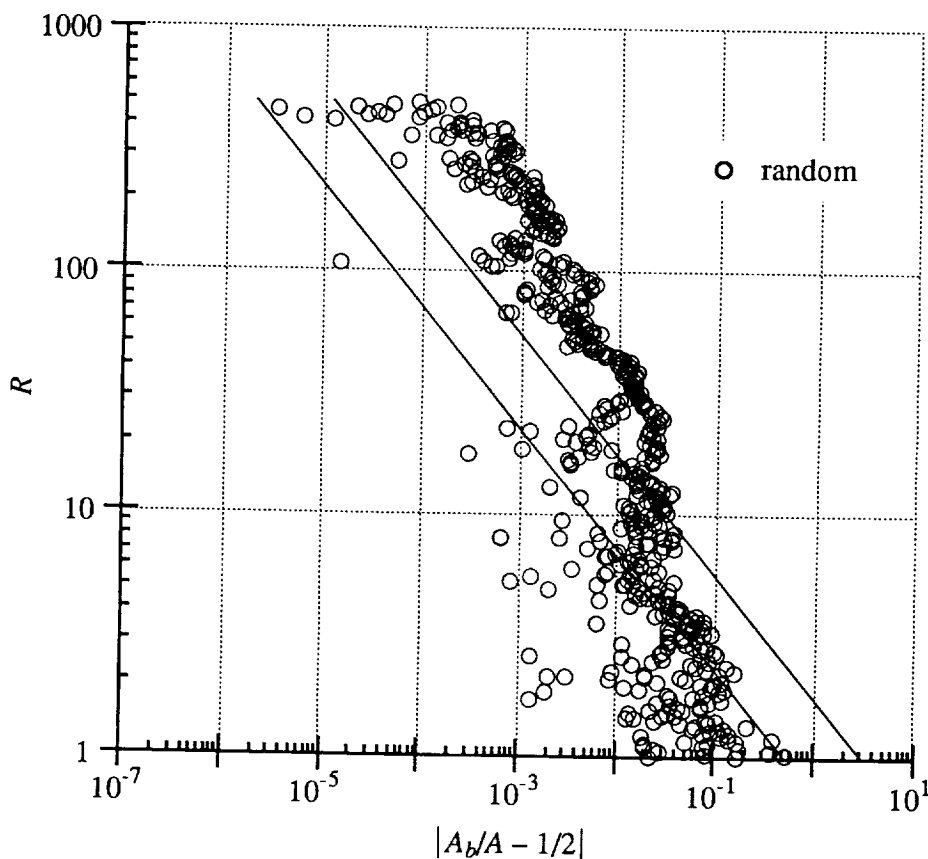


Fig. 3b. Plot of  $(|A_b/A - 1/2|, R)$  pairs for random checkerboard.

### Line Fraction

Next we consider the line fraction  $l_b/l$  of the black phase and study the  $\theta$  and  $l$  dependence of this ratio for the midpoint C fixed at the corner of a black square. As was noted above a naive interpretation of the principle of Delesse would lead one to believe that the ratio  $l_b/l$  should approach the area fraction  $1/2$  as  $l$  increases. However, this is not the case: for instance for the  $45^\circ$  cut  $l_b/l = 1$  for all  $l$  (cf. Fig. 2). Similar results hold for certain other cuts. Indeed, if we let  $m$  be the slope of the line segment ( $m = \tan\theta$ ), we find that for  $0 \leq m \leq 1$

$$\lim_{l \rightarrow \infty} \left( \frac{l_b}{l} \right) = \begin{cases} \frac{1}{2} \left( 1 + \frac{1}{pq} \right) & \text{when } m = \frac{p}{q} \text{ and } p \text{ and } q \text{ are odd and} \\ & \text{have no common divisor other than one} \\ \frac{1}{2} & \text{otherwise} \end{cases} \quad (8)$$

We see from (8) that, in a regular checkerboard, (3) fails to hold for an infinite, but countable number of directions. But, it can be shown that for all macroscopically homogeneous bodies (3) can be replaced by the weaker relation:

$$\int_0^{2\pi} |f_1(x_C, \theta; l) - a_b| d\theta = 0 \quad (9)$$

where  $a_b$  is the area fraction of the black phase.

We continue to study other aspects of the dependence of  $l_b/l$  on  $\theta$  and  $l$  with the aim of shedding further light on the principle of Delesse.

We observe from Fig. 2 that when  $m$  is rational the linear cut has a periodic structure. The period  $L_p$  is given as follows:

$$L_p = \begin{cases} \sqrt{p^2 + q^2} & \text{when } p \text{ and } q \text{ are both even or both odd} \\ 2\sqrt{p^2 + q^2} & \text{otherwise} \end{cases} \quad (10)$$

However, when  $m$  is irrational the cut has a quasi-periodic structure, i.e. the black segments arrange themselves only quasi-periodically over the cut. It is easily seen that this observation can be generalized to higher dimensions. In fact, de Bruijn's (1981) elegant construction of the celebrated quasi-periodic Penrose tilings is based on a three dimensional cut of a five dimensional periodic checkerboard

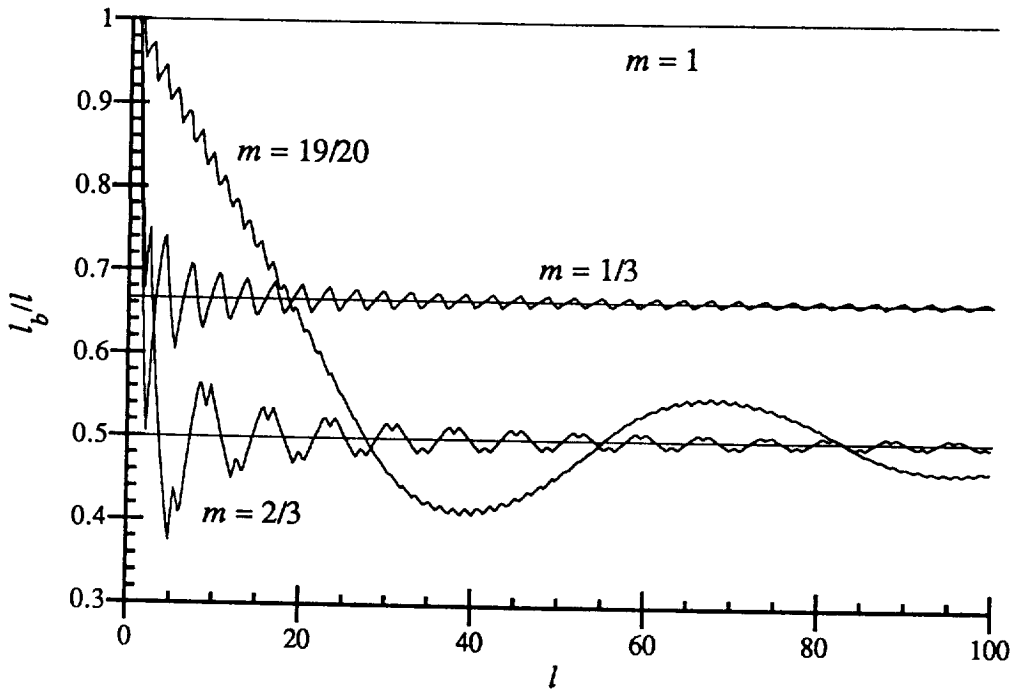


Figure 4.  $l_b/l$  v.  $l$  for fixed  $\theta$  and  $x_C$ .

Fig. 4. shows the dependence of  $l_b/l$  on  $l$  for fixed slopes. It will be noticed that  $l_b/l$  converges to a fixed value as  $l$  increases but that the rate of convergence depends on the period  $L_p$ .

Let  $e$  measure the deviation of  $l_b/l$  from  $1/2$ :

$$e(m, l) = |l_b/l - 1/2| \quad (11)$$

It is clear that  $e$  will depend on the slope  $m$  and the length  $l$  of the segment of measurement and that  $0 \leq e(m, l) \leq 1/2$  by definition.

To summarize the above findings, we calculated the function  $e(m, l)$  at 200,000 evenly spaced points  $(m, l)$ . The results of these calculations are shown in Fig. 5 where the value of  $e$  at a given point is measured by means of a (logarithmic) scale of grayness, a "larger" value of  $e$  corresponding to a darker shading of gray. It will be noticed that the horizontal dark lines in this figure correspond to some of the exceptional values of  $m$  listed in the first line of (8).

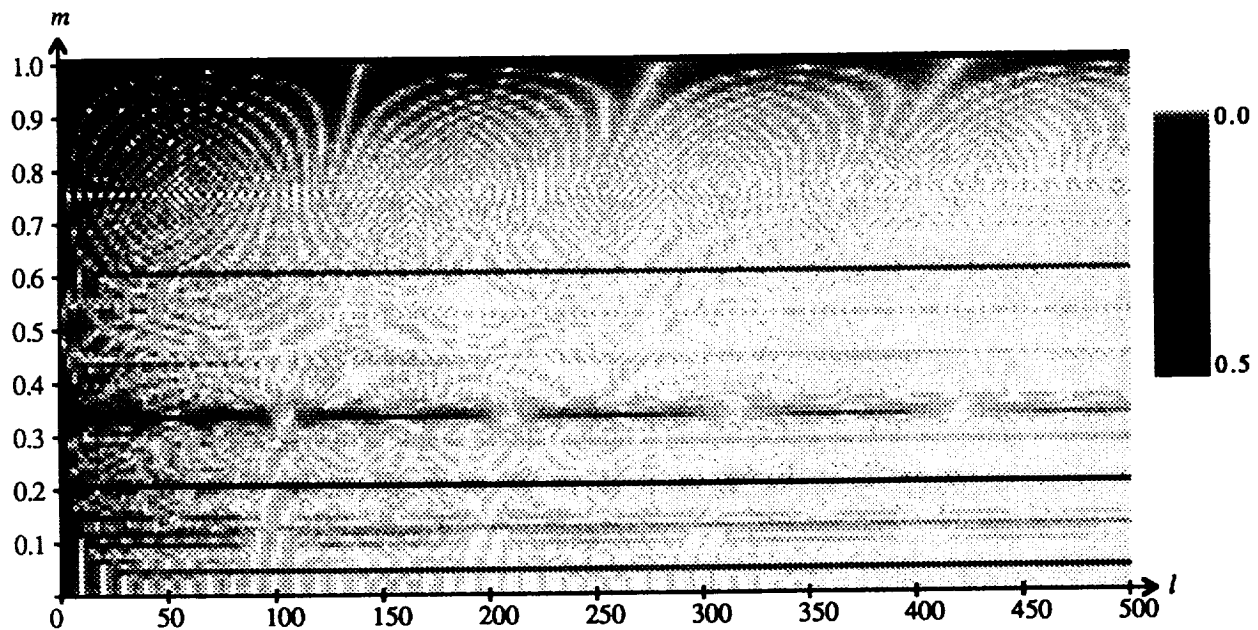


Figure 5. Gray scale plot of  $e(m, l)$ . ( $\Delta m=0.001$  and  $\Delta l=2.5$ )

Fig. 6 is derived from Fig. 5 and exhibits the  $m$  dependence of  $e$  for three fixed values of  $l$ : viz.  $l = 10, 100, \text{ and } 1000$ . The “graphs” for  $l = 10$  and  $100$ , are composed of 1000 discrete points that represent the  $e$  values calculated at 1000 evenly spaced points of the  $m$ -axis. When  $l = 1000$ , the function  $e(m, l = \text{constant})$  exhibits such sharp peaks at the points listed in (8) that the discrete points of evaluation used in the previous figures do not yield a satisfactory “graph” of this function. The  $e$  values calculated at some of these special points were added to the figure for a better description of the  $m$  dependence of  $e$ .

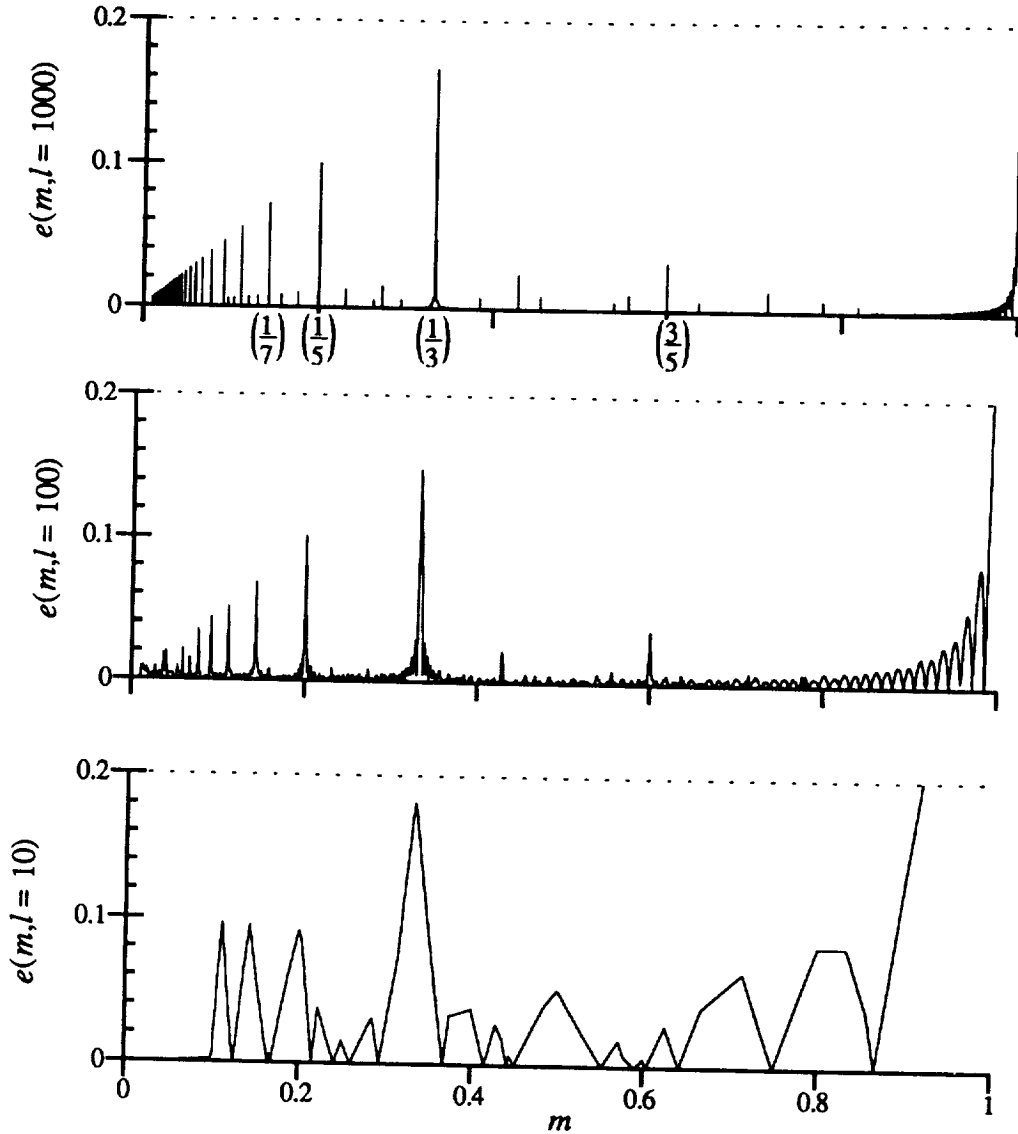


Figure 6.  $l$ -constant sections of  $e(m, l)$ .

We are now ready to return to the Principle of Delesse. We raise the question: what gage length  $l$  should one use in the study of this material in order to obtain a reliable estimate of the area fraction from *one* line fraction measurement? It is clear from (8) and from Fig. 6 that when  $l = 1000$  a random choice of the slope is likely to result in a very good estimate of the area fraction.

In order to be more precise about this statement, we introduce the function  $\text{Pr} \{e > \xi, l\}$  which measures the probability of the error  $e$  exceeding a value  $\xi > 0$  in an observation performed with a line segment of length  $l$  and random slope  $m$ . For each  $l$  and for some  $\xi$  the value of this function was determined from Fig. 6 as follows: first we find the total number of points on the  $m$ -axis amongst the evenly spaced 1000 points, at which the value of  $e$  exceeds  $\xi$  and then normalize this

number by dividing it by 1000 (cf. the case  $l = 10$  in Fig. 5. where a hint is provided concerning the nature of this process).

Fig. 7 shows the  $\xi$  dependence of  $\Pr \{e > \xi, l\}$  for three values of  $l$ . We see that the probability of committing a fixed error  $\xi$  by a bad choice of the slope  $m$  decreases prodigiously as the length of measuring segment increases.

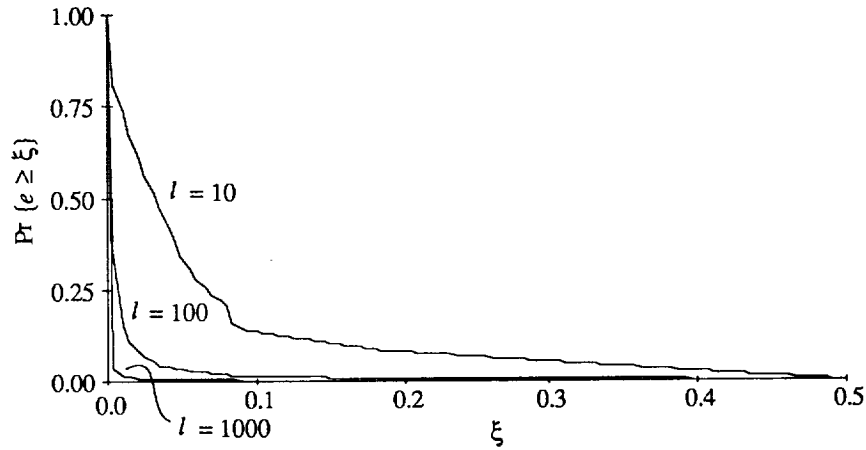


Figure 7. Increasing the gage length decreases the probability of error

All calculations described here were made with line segments which had a common starting point. The influence of the starting point on similar calculations was studied, but we shall not report on these studies because they provide little additional insight.

#### 4. Example: Random Checkerboard

In the above example the microstructure exhibited translational and rotational symmetries and the cell that defined it was small and simple. Here we consider a square checkerboard that has a random microstructure and contains one million black and white elementary squares of size  $1 \times 1$ . The elementary squares are assigned randomly but in such way that the area fraction of the black phase is again  $1/2$ . A sub-region of this random checkerboard is shown in Figure 8. We note that a microstructure that extends to infinity can be created by using copies of this square checkerboard.

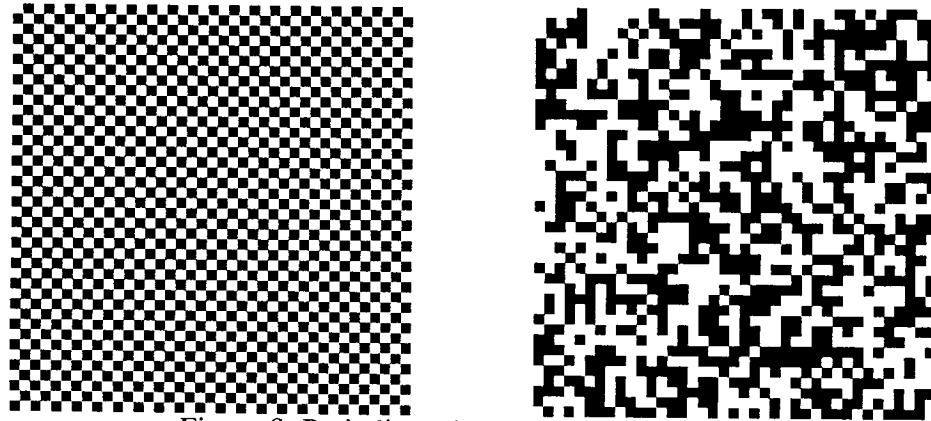


Figure 8. Periodic and random checkerboards.

Area fraction calculations for this structure were performed and are summarized in Fig. 3b. As noted before, in this case a much larger observation window ( $R \geq 50$ ) is needed to estimate the area fraction of the black phase to within an error of 0.01.

We next calculated the line fraction  $l_b/l$  of the black phase by placing an end of the measuring segment at the corner of the random checkerboard. The gray scale plot of the function  $e(m, l)$  which results from these calculations and, as before, measures the deviation of  $l_b/l$  from  $1/2$ , is shown in

Fig. 9.

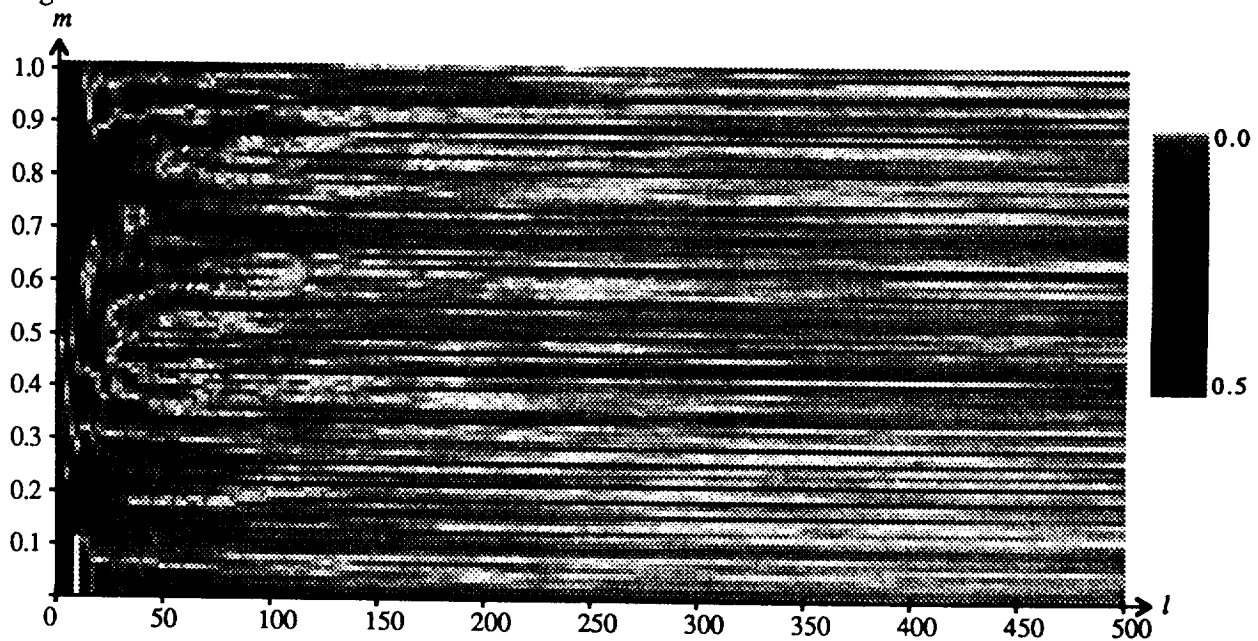


Figure 9. Gray scale plot of  $e(m, l)$  for a random checkerboard ( $\Delta m=0.001$  and  $\Delta l=2.5$ )

The gray scale plot of  $e(m, l)$  for the random checkerboard might suggest to a casual observer that there may be exceptional values of  $m$  at which  $e(m, l)$  does not vanish as  $l$  increases. However, as Fig. 10 shows more clearly, there are no such exceptional values in the case of the random

checkerboard. In this regard Fig. 6 should be compared with Fig. 10. This comparison shows that in the random checkerboard,  $e(m, l)$  decreases with increasing  $l$  for all  $m$ , but that this rate of decrease is very slow compared with the periodic case.

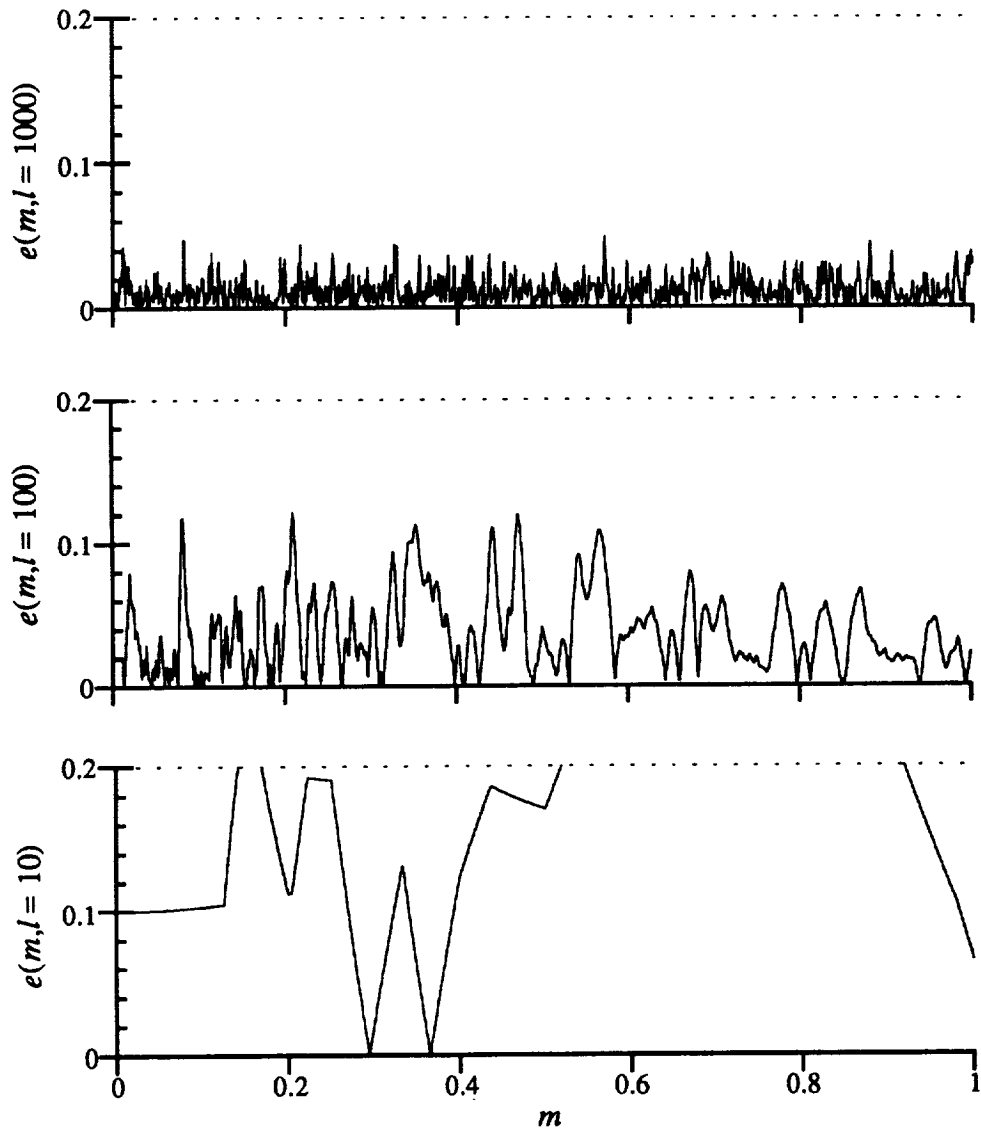


Figure 10.  $l$ -constant sections of  $e(m, l)$  for the random checkerboard.

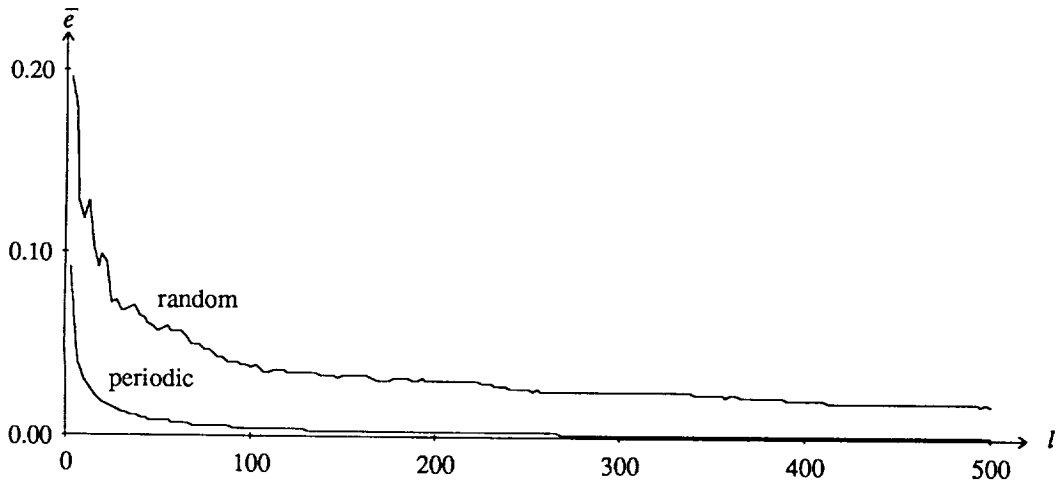


Figure 11.  $e(m, l)$  averaged over  $m$  as a function of  $l$

Fig. 11, which is inspired by (9), provides yet another illustration of this fact.

## 5. Conclusions

We recall that in a *macroscopically homogeneous* material the area fraction of the black phase within a circular observation window will differ from the area fraction  $a_b$  of the material by less than an error of  $\epsilon$ , if the window has a radius larger than the minimal radius  $r(\epsilon)$  (cf. Section 2 ). We find that the function  $r(\epsilon)$  summarizes important facts about the microstructure.

To illustrate this remark, consider, for definiteness, the case where the white phase is connected, the boundary of each black element is smooth and  $a_b \leq 1/2$ . It will then be seen that the diameter of any black element is greater than  $2r(1 - a_b)$ .

As the following examples show, the function  $r(\epsilon)$  also provides a definition and a measure of *clustering* of the elements of microstructure. Consider two macroscopically homogeneous materials that have the same area fraction  $a_b$  and whose black phases are composed of copies of just one disk. As noted before the functions  $r_1(\epsilon)$  and  $r_2(\epsilon)$  for these materials may have widely differing values for some range of  $\epsilon$ .

Reflection will show that the inequality  $r_1(\epsilon) \gg r_2(\epsilon)$  would imply that the black elements in the first material are more clustered. In this regard we refer the reader to the examples discussed in Sections 3 and 4 and to Figs. 3a, 3b and 8. Note that, as Fig. 8 shows, a periodic structure constructed with the smallest cell achieves minimum clustering.

We observed in Section 2 that  $r(\epsilon)$  also provides, in a somewhat definite sense, an estimate of the minimum radius  $R_\epsilon$  which renders the mechanical behavior of a spherical element independent,

to within an error  $\epsilon$ , of the location and size of the element. This is a difficult issue that needs further work.

We discussed, with the help of examples, the  $\theta$  and  $l$  dependence of the function  $f_1(x_C, \theta; l)$  that measures the line fraction of the black phase. These discussions showed that a line fraction measurement could provide a reliable estimate of the area fraction (The principle of Delesse ) if the gage length  $l$  is chosen appropriately. This choice is related to the function  $r(\epsilon)$ . It would be desirable to undertake an analytic study of this relationship.

Line fraction measurements performed at a fixed point  $C$  and with fixed  $l$  define a function on the unit circle of directions. In the periodic checkerboard of Section 3, this function tends to a limit, as  $l \rightarrow \infty$ , which has the value  $a_b$  for all directions except at the ones generated by the list in (8) and its extension. At these exceptional points the limit function assumes the values given in (8). The “spikes” that the graph of this function exhibits (cf. top graph in Fig.6) are a sign that the microstructure has translational symmetries.

It is worth noting that microscopic observations of internal structure of a material often produce functions defined on an object such as a unit circle (as in the above case), unit sphere, etc. Moreover, the Fourier representations of such functions give rise to coefficients that are irreducible tensors (cf. Onat and Leckie (1988)). Thus the tensorial state variables  $(q_1(t), q_2(t), \dots, q_n(t))$ , which describe the changing internal state and orientation for an approximate representation of mechanical behavior, will, in general, be related to these Fourier coefficients that come from measurements of microstructure. A major problem of mechanics of materials is to develop general methods for establishing these relationships. It is also clear that in certain cases the mechanical behavior and, hence,  $q_i(t)$  may not depend at all on the aspects of microstructure studied in a given experiment.

To illustrate these points, consider the simpler task of determining the effective elastic moduli of a macroscopically homogeneous body composed of two homogeneous isotropic elastic materials. Suppose also that we know aspects of the microstructure such as the area fraction  $a_b$ , the function  $r(\epsilon)$  introduced above, and, say, the fact that the line fraction  $f_1$  does not depend on  $x_C$  and  $\theta$  for large  $l$ . It is known that just the knowledge of the elastic properties of the constituents and the area fraction  $a_b$  would enable one to find bounds to the effective moduli of the composite. But in certain cases these bounds cannot be close to each other. Indeed if  $a_b = 1/2$  and if one of the phases is *connected* and less stiff than the other one, then the switching of materials between phases would not change  $a_b$  but could create a stiffer composite, indicating that the bounds to the effective moduli may not be close to each other in this case. Note, however, that the switching of materials will, in general, change the function  $r(\epsilon)$ . We may therefore hope that a calculation of the effective moduli which takes into account this microstructural information might produce better results. Nevertheless we believe that for still better results one will need to introduce into analysis

parameters that measure the presence and the strength of connectivity and its strength in constituent phases.

### **References**

Delesse, M.A. *C. R. Acad. Sci. (Paris)* **25**, 544 (1847).

Weibel, E. R. *Stereological Methods* Vol.2, Academic Press, (1980 )

Bruijn, N.G. de *Proceedings Dutch Academy of Science A* **84** (1), 39 (1981).

Geary, J. E. and E. T. Onat. *Oak Ridge National Laboratory Report ORNL-TM-4525*, (1974)

Onat, E. T. and F. A. Leckie, *Journal of Applied Mechanics* **110**, March,1 (1988)

### **Acknowledgement**

This work was supported by a grant from the National Aeronautics and Space Administration.

The date of work: 24 July 1990.



National Aeronautics and  
Space Administration

## Report Documentation Page

1. Report No. NASA CR - 187130		2. Government Accession No.		3. Recipient's Catalog No.	
4. Title and Subtitle On Representation of Mechanical Behavior and Stereological Measures of Microstructure				5. Report Date June 1991	
				6. Performing Organization Code	
7. Author(s) E.T. Onat and S.I. Wright				8. Performing Organization Report No. None	
				10. Work Unit No. 510-01-50	
9. Performing Organization Name and Address Yale University Department of Mechanical Engineering New Haven, Connecticut 06520-2157				11. Contract or Grant No. NAG3-834	
				13. Type of Report and Period Covered Contractor Report Final	
12. Sponsoring Agency Name and Address National Aeronautics and Space Administration Lewis Research Center Cleveland, Ohio 44135-3191				14. Sponsoring Agency Code	
15. Supplementary Notes Project Manager, Steven M. Arnold, Structures Division, NASA Lewis Research Center, (216) 433-3334.					
16. Abstract Macroscopic homogeneity of a heterogeneous body is defined from various points of view. The applicability of the principle of Delesse to a single macroscopically homogeneous body is discussed. It is then seen that a function derived from a consideration of the area fraction of a phase can serve as a measure of clustering of particles of that phase.					
17. Key Words (Suggested by Author(s)) Homogenization Continuum mechanics Heterogeneity			18. Distribution Statement Unclassified - Unlimited Subject Category 39		
19. Security Classif. (of the report) Unclassified		20. Security Classif. (of this page) Unclassified		21. No. of pages 20	22. Price* A03